

Quark deconfinement in high-mass neutron stars

M. Orsaria,^{1,2,*} H. Rodrigues,^{3,†} F. Weber,^{4,5,‡} and G. A. Contrera^{6,7,8,§}

¹*Department of Physics, San Diego State University,
5500 Campanile Drive, San Diego, CA 92182, USA*

²*CONICET, Rivadavia 1917, 1033 Buenos Aires, Argentina;
Gravitation, Astrophysics and Cosmology Group,
Facultad de Ciencias Astronómicas y Geofísicas, UNLP,
Paseo del Bosque S/N (1900), La Plata, Argentina*

³*Centro Federal de Educação Tecnológica do Rio de Janeiro,
Av Maracanã 249, 20271-110, Rio de Janeiro, RJ, Brazil*

⁴*Department of Physics, San Diego State University,
5500 Campanile Drive, San Diego, California 92182*

⁵*Center for Astrophysics and Space Sciences, University of California,
San Diego, La Jolla, CA 92093, USA*

⁶*CONICET, Rivadavia 1917, 1033 Buenos Aires, Argentina*

⁷*IFLP, CONICET - Dpto. de Física, UNLP, La Plata, Argentina,*

⁸*Gravitation, Astrophysics and Cosmology Group,
Facultad de Ciencias Astronómicas y Geofísicas, UNLP,
Paseo del Bosque S/N (1900), La Plata, Argentina*

Abstract

In this paper, we explore whether or not quark deconfinement may occur in high-mass neutron stars such as J1614-2230 ($1.97 \pm 0.04 M_{\odot}$) and J0348+0432 ($2.01 \pm 0.04 M_{\odot}$). Our study is based on a non-local extension of the SU(3) Nambu Jona-Lasinio (n3NJL) model with repulsive vector interactions among the quarks. This model goes beyond the frequently used local version of the Nambu Jona-Lasinio (NJL) model by accounting for several key features of QCD which are not part of the local model. Confined hadronic matter is treated in the framework of non-linear relativistic mean field theory. We find that both the local as well as the non-local NJL model predict the existence of extended regions of mixed quark-hadron (quark-hybrid) matter in high-mass neutron stars with masses of 2.1 to 2.4 M_{\odot} . Pure quark matter in the cores of neutron stars is obtained for certain parametrizations of the hadronic lagrangian and choices of the vector repulsion among quarks. The radii of high-mass neutron stars with quark-hybrid matter and/or pure quark matter cores in their centers are found to lie in the canonical range of 12 to 13 km.

PACS numbers: 97.60.Jd, 21.65.Qr, 25.75.Nq, 26.60.Kp

* morsaria@rohan.sdsu.edu

† harg@cefet-rj.br

‡ fweber@mail.sdsu.edu

§ guscontrera@gmail.com

I. INTRODUCTION

White dwarf and neutron stars (NSs) are born in the aftermath of core-collapsing supernova explosions. Depending on NS mass and rotational frequency, gravity may compress the matter in the core regions of such stars up to more than ten times the density of ordinary atomic nuclei, thus providing a high-pressure environment in which numerous subatomic particle processes are likely to compete with each other. Theoretical studies indicate that hyperons, boson condensates (pions, kaons, H-matter) and/or deconfined up, down and strange quarks may exist in the core regions of NSs (for an overview, see [1–12] and references therein).

Based on qualitative considerations concerning the stiffness of the nuclear equation of state (EoS), one could argue that the detection of high-mass NSs, such as PSR J1614–2230 with a gravitational mass of $1.97 \pm 0.04 M_{\odot}$ [14] and PSR J0348+0432 with a mass of $2.01 \pm 0.04 M_{\odot}$ [15], may rule out the existence of deconfined quarks in their central core regions, since quark deconfinement would take away so much pressure that high-mass NSs are not supported. As shown in Ref. [16], conclusions of that kind are not necessarily correct.

Our paper builds on the investigations carried out in Ref. [16] for NSs containing deconfined quark matter, i.e. quark-hybrid stars (QHSs). The study is based on a generalized version of the Nambu Jona-Lasinio (NJL) model [17], which accounts for several basic properties of quantum chromodynamics (QCD). As an improvement of the standard NJL model, we will consider non-local interactions among the quarks [18]. By combining the NJL model and the one-gluon-exchange model, which uses an effective gluon propagator to model effective interactions among the quarks, it is possible to introduce the non-locality in the quark-quark interaction [19] through a model-dependent form factor $g(p)$, in a natural way. Table I compares the key features of the standard (local) NJL with those of the non-local NJL model. Advantages of the non-local model over the local model are indicated.

SU(2) versions of the nonlocal NJL model have been applied to the study of hybrid stars in the past [20–22]. In this work, we model the quark phase that may exist in the core of a neutron star using the non-local 3-flavor NJL (n3NJL) model of Refs. [26] and [27], which includes vector interactions among the quarks. In our previous work [16], we considered the vector interaction of the non-local NJL model in a phenomenological way, and found that the transition to pure quark matter occurs only in neutron stars which lie already on

Table I. Comparison of the key features of the local and non-local NJL model.

Local NJL	Non-local NJL model
• Lack of confinement.	• Confinement with a proper choice of the non-local regulator and model parameters [23].
• Quark-quark scalar-isoscalar and pseudoscalar-isovectorial local interaction.	• Quark-quark interaction through phenomenologically (effective) quark propagator.
• Non-renormalizable. Ultra-violet (UV) cutoff (Λ) is needed.	• UV divergences are fixed [18]. Model dependent form factor $g(p)$.
• Dynamical quark masses are momentum independent.	• Dynamical quark masses are momentum dependent (as also found in lattice QCD calculations) [24].
• Divergences in the meson loop integrals. Extra cutoffs are needed.	• The momentum dependent regulator makes the theory finite to all orders in the $1/N_c$ expansion [25].
• The Λ cutoff is turned off at high momenta, limiting the applicability of the model at high densities.	• The form factor provides a natural cutoff that falls off at high momenta.

the gravitationally unstable branch of the stellar sequence. In this paper, we explore the effect of the shift of the chemical potential on the form factor, when vector interactions are considered. The results are compared with those obtained by modeling the quark phase in the framework of the local SU(3) NJL model (l3NJL) described, for example, in Refs. [28–31]. The vector interactions are known to be important for the QCD phase diagram [32]. It is therefore interesting, if not mandatory, to explore the consequences of the vector interactions for the EoS of neutron star matter and the structure of compact stars computed for such EoSs.

Global electric charge neutrality is imposed on the constituents of neutron star matter.

Local NJL studies carried out for local electric charge neutrality have been reported recently in Refs. [33, 34, 39]. In [33] a non-linear Walecka model was employed for the hadronic phase, using parametrizations GM1 [40] and NL3 [41], and the local NJL model for the quark phase. In that work it was found that the observation of compact stars with masses greater than around $2 M_{\odot}$ would be hard to explain unless one uses a very stiff hadronic model for the nuclear EoS, such as NL3 with nucleons only, instead of the softer GM1 EoS. The authors in reference [34] treat vector interactions and color superconductivity among the quarks in the framework of the local NJL model, using the NL3 and GM3 parametrizations for the description of confined hadronic matter. The maximum mass of a neutron star was found to exceed $2 M_{\odot}$. A possible mixed phase of quarks and hadrons has not been considered in [34], whose appearance depends on the surface tension between nuclear matter and quark matter, which is only very poorly known [1, 35–37]. Screening and surface tension may be very important for understanding the quark-hadron phase transition and the existence of the mixed phase [35].

The authors in [38] analyze the possibility of quark matter nucleation in high-mass neutron stars using the non-linear Walecka model plus the local NJL model with vector interaction for the EoS. They obtain stable NSs configurations with quark cores when the NL3 parametrization is considered (being $2.18 M_{\odot}$ the largest NS mass) and NSs with mixed phase in their centers if the parametrization for the hadronic phase is TM1 or TM2 (being $2.03 M_{\odot}$ the maximum star mass).

Finally, we mention the study of Ref. [39], where it was found on the basis of the percolation picture from the hadronic phase with hyperons to the quark phase with strangeness that massive neutron stars with quark matter cores are compatible with the mass observed for PSR J1614–2230, provided the crossover from hadronic matter to quark matter takes place at around three times the normal nuclear matter density, quark matter is strongly interacting in the crossover region, and has a stiff equation of state.

This work is organized as follows. In Sect. II, we describe the local as well as the non-local extension of the SU(3) NJL model at zero temperature. In Sect. III, the non-linear relativistic Walecka model, which is used to model confined hadronic matter, is briefly discussed. In Sect. IV, we analyze the construction of the mixed quark-hadron phase subjected to global electric charge neutrality. Our results for the quark-hadron composition and bulk properties of neutron stars are presented in Sects. V and VI. Finally, a summary and discussion of our

results is provided in Sect. VII.

II. QUARK MATTER PHASE

A. The local 3-flavor NJL model with vector interaction (l3NJL)

As an effective model of QCD, the NJL model accounts for the interactions between constituent quarks and provides a simple scheme for studying spontaneous chiral symmetry breaking, a key feature of quantum chromodynamics (QCD) in the low temperature and density domain, and its manifestations in hadron physics, such as dynamical quark mass generation, the appearance of quark pair condensates, and the role of pions as Goldstone bosons. The effective action of the local 3-flavor NJL model with vector interaction (l3NJL) used in this paper is given by

$$S_E = \int d^4x \left\{ \bar{\psi}(x)(i\partial - \hat{m})\psi(x) + \frac{1}{2} G_S [(\bar{\psi}(x)\lambda_a\psi(x))^2 + (\bar{\psi}(x)i\gamma_5\lambda_a\psi(x))^2] \right. \\ \left. + H [\det[\bar{\psi}(x)(1 + \gamma_5)\psi(x)] + \det[\bar{\psi}(x)(1 - \gamma_5)\psi(x)]] \right. \\ \left. - G_V [(\bar{\psi}(x)\gamma^\mu\lambda_a\psi(x))^2 + (\bar{\psi}(x)i\gamma^\mu\gamma_5\lambda_a\psi(x))^2] \right\}, \quad (1)$$

where ψ is a chiral U(3) vector that includes the light quark fields, $\psi \equiv (u, d, s)^T$, $\hat{m} = \text{diag}(m_u, m_d, m_s)$ is the current quark mass matrix, λ_a with $a = 1, \dots, 8$ denote the generators of SU(3), and $\lambda_0 = \sqrt{2/3} \mathbb{1}_{3 \times 3}$. The values for the coupling constants G_S and H as well as the strange quark mass m_s and the three-momentum ultraviolet cutoff parameter, Λ , are model parameters. Their values are taken from Ref. [29], i.e., $m_u = m_d = 5.5$ MeV, $m_s = 140.7$ MeV, $\Lambda = 602.3$ MeV, $G_S\Lambda^2 = 3.67$ and $H\Lambda^5 = -12.36$. The vector coupling constant G_V is treated as a free parameter.

At the mean-field level, the thermodynamic potential associated with S_E is given by

$$\Omega^L(M_f, \mu) = G_S \sum_{f=u,d,s} \langle \bar{\psi}_f \psi_f \rangle^2 + 4H \langle \bar{\psi}_u \psi_u \rangle \langle \bar{\psi}_d \psi_d \rangle \langle \bar{\psi}_s \psi_s \rangle - 2N_c \sum_{f=u,d,s} \int_\Lambda \frac{d^3p}{(2\pi)^3} E_f \\ - \frac{N_c}{3\pi^2} \sum_{f=u,d,s} \int_0^{p_{Ff}} dp \frac{p^4}{E_f} - G_V \sum_f \rho_f^2, \quad (2)$$

where $N_c = 3$, $E_f = \sqrt{\mathbf{p}^2 + M_f^2}$, and $p_{F_f} = \sqrt{\mu_f^2 - M_f^2}$. The constituent quark masses M_f are given by

$$M_f = m_f - 2G_S \langle \bar{\psi}_f \psi_f \rangle - 2H \langle \bar{\psi}_j \psi_j \rangle \langle \bar{\psi}_k \psi_k \rangle, \quad (3)$$

with $f, j, k = u, d, s$ indicating cyclic permutations. The vector interaction shifts the quark chemical potential according to

$$\mu_f \rightarrow \mu_f - 2G_V \rho_f, \quad (4)$$

where ρ_f is the quark number density corresponding to the flavor f in the mean field approximation, that is,

$$\rho_f = \frac{N_c}{3\pi} [(\mu_f - 2G_V \rho_f)^2 - M_f^2]^{3/2}. \quad (5)$$

The quark condensates $\langle \bar{\psi}_f \psi_f \rangle$ can be determined by minimizing the thermodynamic potential as $\langle \bar{\psi}_f \psi_f \rangle$, that is,

$$\frac{\partial \Omega^L}{\partial \langle \bar{\psi}_f \psi_f \rangle} = 0, \quad f = u, d, s. \quad (6)$$

B. The non-local 3-flavor model with vector interaction (n3NJL)

In this section we briefly describe the non-local extension of the SU(3) Nambu Jona-Lasinio (n3NJL) model. The Euclidean effective action for the quark sector, including the vector interaction, is given by

$$S_E = \int d^4x \left\{ \bar{\psi}(x) [-i\partial + \hat{m}] \psi(x) - \frac{G_S}{2} [j_a^S(x) j_a^S(x) + j_a^P(x) j_a^P(x)] \right. \\ \left. - \frac{H}{4} T_{abc} [j_a^S(x) j_b^S(x) j_c^S(x) - 3 j_a^S(x) j_b^P(x) j_c^P(x)] - \frac{G_V}{2} [j_V^\mu(x) j_V^\mu(x)] \right\}, \quad (7)$$

where ψ and \hat{m} stand for the light quark fields and the current quark mass matrix, respectively. For simplicity, we consider the isospin symmetric limit in which case $m_u = m_d = \bar{m}$. The operator $\partial = \gamma_\mu \partial_\mu$ in Euclidean space is defined as $\vec{\gamma} \cdot \vec{\nabla} + \gamma_4 \frac{\partial}{\partial \tau}$, with $\gamma_4 = i\gamma_0$. The Scalar, Pseudoscalar $j_a^{S,P}(x)$ and $j_V^\mu(x)$ vector currents are, respectively, given by

$$j_a^S(x) = \int d^4z \tilde{g}(z) \bar{\psi} \left(x + \frac{z}{2} \right) \lambda_a \psi \left(x - \frac{z}{2} \right), \\ j_a^P(x) = \int d^4z \tilde{g}(z) \bar{\psi} \left(x + \frac{z}{2} \right) i \gamma_5 \lambda_a \psi \left(x - \frac{z}{2} \right), \\ j_V^\mu(x) = \int d^4z \tilde{g}(z) \bar{\psi} \left(x + \frac{z}{2} \right) \gamma^\mu \lambda_a \psi \left(x - \frac{z}{2} \right), \quad (8)$$

where $\tilde{g}(z)$ is a form factor responsible for the non-local character of the interaction and λ_a represent the generators of SU(3), as for the local model.

Finally, the constants T_{abc} in the t'Hooft term, which account for flavor-mixing, are defined by

$$T_{abc} = \frac{1}{3!} \epsilon_{ijk} \epsilon_{mnl} (\lambda_a)_{im} (\lambda_b)_{jn} (\lambda_c)_{kl} . \quad (9)$$

After standard bosonization of Eq. (7), the integrals over the quark fields can be evaluated in the framework of the Euclidean four-momentum formalism. The thermodynamic potential, in the mean-field approximation at zero temperature, can then be written as

$$\begin{aligned} \Omega^{NL}(M_f, 0, \mu_f) = & -\frac{N_c}{\pi^3} \sum_{f=u,d,s} \int_0^\infty dp_0 \int_0^\infty dp \ln \left\{ [\hat{\omega}_f^2 + M_f^2(\omega_f^2)] \frac{1}{\omega_f^2 + m_f^2} \right\} \\ & -\frac{N_c}{\pi^2} \sum_{f=u,d,s} \int_0^{\sqrt{\mu_f^2 - m_f^2}} dp p^2 [(\mu_f - E_f)\theta(\mu_f - m_f)] \\ & -\frac{1}{2} \left[\sum_{f=u,d,s} (\bar{\sigma}_f \bar{S}_f + \frac{G_S}{2} \bar{S}_f^2) + \frac{H}{2} \bar{S}_u \bar{S}_d \bar{S}_s \right] - \sum_{f=u,d,s} \frac{\varpi_f^2}{4G_V}, \end{aligned} \quad (10)$$

where $N_c = 3$, $E_f = \sqrt{p^2 + m_f^2}$, and $\omega_f^2 = (p_0 + i\mu_f)^2 + p^2$. The constituent quark masses M_f are treated as momentum-dependent quantities and are given by

$$M_f(\omega_f^2) = m_f + \bar{\sigma}_f g(\omega_f^2), \quad (11)$$

where $g(\omega_f^2)$ is the Fourier transform of the form factor $\tilde{g}(z)$. The inclusion of vector interactions shifts the quark chemical potential as

$$\mu_f \rightarrow \hat{\mu}_f = \mu_f - g(\omega_f^2) \varpi_f, \quad (12)$$

where ϖ_f represent the vector mean fields related to the vector current interaction (last term in Eq. (7)). The inclusion of the form factor in Eq. (12) is a particular feature of the non-local model, which renders the shifted chemical potential momentum dependent. Accordingly, the four momenta ω_f in the dressed part of the thermodynamic potential are modified as

$$\omega_f^2 \rightarrow \hat{\omega}_f^2 = (p_0 + i\hat{\mu}_f)^2 + p^2. \quad (13)$$

We followed the prescriptions given in [20] to include the vector interaction. Note that the quark chemical potential shift does not affect the non-local form factor $g(\omega_f^2)$, as discussed in [20, 42, 43], avoiding a recursive problem.

As we mentioned before, the form factor $\tilde{g}(z)$ is defined by its Fourier transform in Euclidean space, which we take to be Gaussian

$$g(\omega_f^2) = \exp(-\omega_f^2/\Lambda^2). \quad (14)$$

It is worth noting that in Eq.14, Λ is not a cutoff as in the case of the local NJL, but a model parameter which plays a role for the width of the chiral transition. This parameter as well as the quark current masses and coupling constants in Eq. (7) can be chosen so as to reproduce the phenomenological values of pion decay constant f_π , and the meson masses

Table II. Parameters used for the non-local NJL (n3NJL) model calculations presented in this paper.

Parameters	n3NJL
\bar{m}	6.2 MeV
m_s	140.7 MeV
Λ	706.0 MeV
$G_S\Lambda^2$	15.04
$H\Lambda^5$	-337.71

m_π , m_η , $m_{\eta'}$, as described in Refs. [26, 27]. In this work we use for the n3NJL model the parameters listed in Table II [16].

Within the stationary phase approximation, the mean-field values of the auxiliary fields \bar{S}_f turn out to be related to the mean-field values of the scalar fields $\bar{\sigma}_f$ [44]. They are given by

$$\bar{S}_f = -16 N_c \int_0^\infty dp_0 \int_0^\infty \frac{dp}{(2\pi)^3} g(\omega_f^2) \frac{M_f(\omega_f^2)}{\hat{\omega}^2 + M_f^2(\omega_f^2)}. \quad (15)$$

The mean field values of $\bar{\sigma}_u$, $\bar{\sigma}_s$ and ϖ_f are obtained via minimizing the thermodynamic potential,

$$\frac{\partial \Omega^{NL}}{\partial \bar{\sigma}_f} = 0, \quad \frac{\partial \Omega^{NL}}{\partial \varpi_f} = 0. \quad (16)$$

III. HADRONIC MATTER PHASE

The hadronic phase is described in the framework of non-linear relativistic field theory [45, 46], where baryons (neutrons, protons, hyperons, delta states) interact via the exchange

of scalar, vector and isovector mesons (σ , ω , ρ , respectively). The parametrizations used in our study are GM1 [40] and NL3 [41]. The associated parameter values are summarized in Table III.

The total lagrangian of the model is given by [1, 2]

$$\mathcal{L} = \mathcal{L}_H + \mathcal{L}_\ell, \quad (17)$$

with the leptonic lagrangian given by

$$\mathcal{L}_\ell = \sum_{\lambda=e^-, \mu^-} \bar{\psi}_\lambda (i\gamma_\mu \partial^\mu - m_\lambda) \psi_\lambda. \quad (18)$$

The hadronic lagrangian in Eq. (17) has the form

$$\begin{aligned} \mathcal{L}_H = & \sum_{B=n,p,\Lambda,\Sigma,\Xi,\Delta} \bar{\psi}_B [\gamma_\mu (i\partial^\mu - g_\omega \omega^\mu - g_\rho \vec{\rho}_\mu) - (m_N - g_\sigma \sigma)] \psi_B \\ & + \frac{1}{2} (\partial_\mu \sigma \partial^\mu \sigma - m_\sigma^2 \sigma^2) - \frac{1}{3} b_\sigma m_N (g_\sigma \sigma)^3 - \frac{1}{4} c_\sigma (g_\sigma \sigma)^4 \\ & - \frac{1}{4} \omega_{\mu\nu} \omega^{\mu\nu} + \frac{1}{2} m_\omega^2 \omega_\mu \omega^\mu + \frac{1}{2} m_\rho^2 \vec{\rho}_\mu \cdot \vec{\rho}^\mu - \frac{1}{4} \vec{\rho}_{\mu\nu} \vec{\rho}^{\mu\nu}. \end{aligned} \quad (19)$$

The quantity B sums all baryonic particles which are produced in neutron star matter at a given density [1, 2]. Intriguingly (see Sect. VI), we find that, in addition to hyperons, the Δ^- particle is generated in neutron star matter at densities which are relevant for stable neutron stars. In contrast to this, treatments of the quark-hadron phase transition based on the MIT bag model [36, 37] do not predict the occurrence of the Δ^- state.

The quantities g_ρ , g_σ , and g_ω in Eq. (19) are meson-baryon coupling constants whose values are summarized in Table III.

Table III. Parameters of the hadronic lagrangian of Eq. (19).

Coupling constants	Parametrizations	
	GM1	NL3
g_σ	8.910	10.217
g_ω	10.610	12.868
g_ρ	8.196	8.948
b_σ	0.002947	0.002055
c_σ	-0.001070	-0.002651

Table IV. Properties of symmetric nuclear matter at saturation density for the parameters listed in Table III. Shown are the saturation density ρ_0 , energy per baryon E/N , nuclear incompressibility K , effective nucleon mass m_N^* , and asymmetry energy a_{sy} .

Properties	Parametrizations	
	GM1	NL3
ρ_0 (fm^{-3})	0.153	0.148
E/N (MeV)	-16.3	-16.3
K (MeV)	300	272
m^*/m_N	0.78	0.60
a_{sy} (MeV)	32.5	37.4

Table IV lists the properties of symmetric nuclear matter computed from Eq. (19) for the relativistic mean-field approximation. The most important differences between the three parameter sets concern the values of the nuclear incompressibility and the asymmetry energy. The maximum neutron star masses for GM1 and NL3 are $2.23 M_\odot$ and $2.77 M_\odot$, respectively, for confined hadronic matter. This is illustrated in Fig. 1, which shows the mass-radius

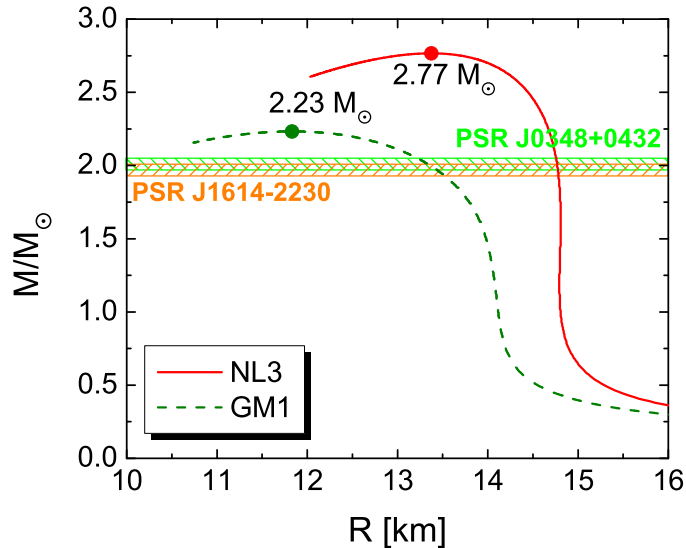


Figure 1. (Color online) Mass-radius relationships of neutron stars computed for the pure (no quark matter) hadronic EoS studied in this work.

relationship of neutron stars for the parametrizations (Table III) studied in this work.

IV. QUARK-HADRON MIXED PHASE

The basic particle reactions in chemically equilibrated quark matter are given by the strong process $u + d \leftrightarrow u + s$ and the weak processes $d(s) \rightarrow u + e^-$ and $u + e^- \rightarrow d(s)$. Neutrinos, once created by the weak reactions, do not accumulate in cold neutron star matter, which implies zero chemical potentials for (anti) neutrinos. The chemical potential for each quark flavor f is then given by

$$\mu_f = \mu_b - Q_f \mu_e, \quad (20)$$

where μ_b and μ_e denote the baryon and electron chemical potential, respectively, and Q_f stand for the electric charge of a quark of flavor f . The baryon chemical potential is related to the quark chemical potentials according to $\mu_b = 1/3 \sum_f \mu_f$.

The contribution of the leptons present in the quark matter phase to the thermodynamic potential is given by

$$\Omega_{\lambda=e^-, \mu^-}(\mu_e) = -\frac{1}{\pi^2} \int_0^{p_{F_\lambda}} p^2 \left(\sqrt{p^2 + m_\lambda^2} - \mu_e \right) dp. \quad (21)$$

Muons occur in the system if the electron chemical potential $\mu_e = \mu_\mu$ is greater than the muon rest mass, $m_\mu = 105.7$ MeV. For electrons we have $m_e = 0.511$ MeV. For the l3NJL model, the total thermodynamic potential for the quark phase is then given by Eqs. (2) and (21). For the n3NJL model, the total thermodynamic potential follows from Eqs. (10) and (21).

If the dense interior of a neutron star is indeed converted to quark matter, it must be three-flavor quark matter since it has lower energy than two-flavor quark matter. And just as for the hyperon content of neutron stars, strangeness is not conserved on macroscopic time scales, which allows neutron stars to convert confined hadronic matter to three-flavor quark matter until equilibrium brings this process to a halt. As first realized by Glendenning [1, 36, 37], the presence of quark matter in neutron stars enables the hadronic regions of the mixed phase to become more isospin symmetric than in the pure phase by transferring electric charge to the quark phase. The symmetry energy can be lowered thereby at only a small cost in rearranging the quark Fermi surfaces. The electrons play only a minor role when neutrality can be achieved among the baryon-charge carrying particles. The stellar implication of this charge rearrangement is that the mixed phase region of a neutron star will

have positively charged regions of nuclear matter and negatively charged regions of quark matter [1, 36, 37]. This should have important implications for the electric and thermal properties of neutron stars. First studies of the transport properties of quark-hybrid neutron star matter have been reported in [47, 48].

To determine the mixed phase region of quarks and hadrons, we start from the Gibbs condition for pressure equilibrium between confined hadronic (P^H) matter and deconfined quark (P^q) matter. The Gibbs condition is given by [1, 36, 37]

$$P^H(\mu_b^H, \mu_e^H, \{\phi\}) = P^q(\mu_b^q, \mu_e^q, \{\psi\}), \quad (22)$$

with $\mu_b^H = \mu_b^q$ for the baryon chemical potentials and $\mu_e^H = \mu_e^q$ for the electron chemical potentials in the hadronic (H) and quark (q) phase, respectively. By definition, the quark chemical potential is given by $\mu_b^q = \mu_n/3$, where μ_n is the chemical potential of the neutron. The quantities $\{\phi\}$ and $\{\psi\}$ in Eq. (22) stand collectively for the field variables and Fermi momenta that characterize the solutions to the equations of confined hadronic matter and deconfined quark matter, respectively. In the mixed phase, the baryon number density, n_b , and the energy density, ε , are given by [1, 36, 37]

$$n_b = (1 - \chi)n_b^H + \chi n_b^q, \quad (23)$$

and

$$\varepsilon = (1 - \chi)\varepsilon^H + \chi\varepsilon^q, \quad (24)$$

where n_b^H (ε^H) and n_b^q (ε^q) denote the baryon number (energy) densities of the hadron and quark phase, respectively. The quantity $\chi \equiv V_q/V$ denotes the volume proportion of quark matter, V_q , in the unknown volume V . By definition, χ therefore varies between 0 and 1, depending on how much confined hadronic matter has been converted to quark matter [1, 36, 37]. In addition to the Gibbs condition (22) for pressure, the conditions of global baryon number conservation and global electric charge neutrality need to be imposed on the field equations. The global conservation of baryon charge is expressed as [1, 36, 37]

$$\rho_b = \chi \rho_Q(\mu_n, \mu_e) + (1 - \chi) \rho_H(\mu_n, \mu_e, \{\phi\}), \quad (25)$$

where ρ_Q and ρ_H denote the baryon number densities of the quark phase and hadronic phase, respectively. The condition of global electric charge neutrality is given by the equation

$$(1 - \chi) \sum_{i=B,l} q_i^H n_i^H + \chi \sum_{i=q,l} q_i^q n_i^q = 0, \quad (26)$$

where q_i is the electric charge of the i -th specie in units of the electron charge. In this work we have chosen global rather than local electric charge neutrality. The latter is not fully consistent with the Einstein-Maxwell equations and the micro physical condition of chemical equilibrium and relativistic quantum statistics, as shown in [49]. In contrast to local electric charge neutrality, the global neutrality condition puts a net positive electric charge on confined hadronic matter, rendering it more isospin symmetric, and a net negative electric charge on the deconfined quark phase, allowing neutron star matter to settle down in a lower energy state than otherwise possible [36, 37].

V. MODELS FOR THE ULTRA-DENSE PART OF THE EOS OF NEUTRON STAR MATTER

Figures 2 and 3 show the EoS of neutron star matter computed for the local (l3NJL) and non-local (n3NJL) model, respectively. The hadronic contributions are computed for the lagrangian given in Eq. (17). For the quark matter phase the local NJL model (Sec. II A) and the non-local NJL model (Sec. II B) have been used. For the hadronic phase

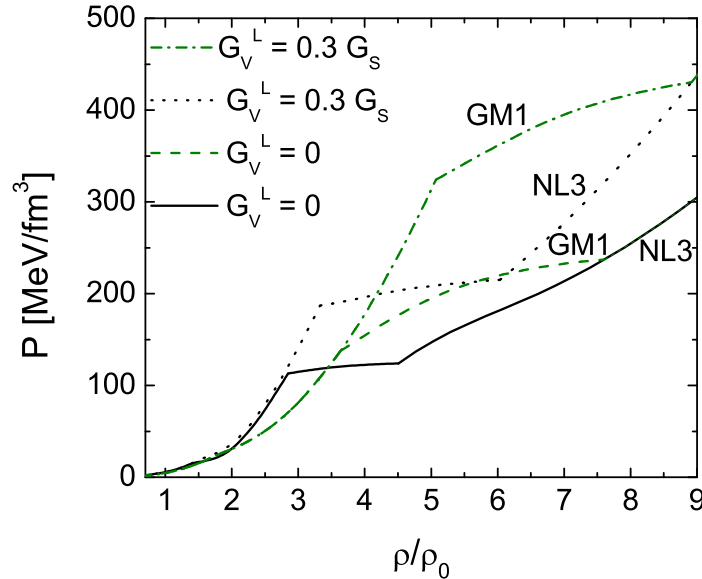


Figure 2. (Color online) Pressure as a function of baryon number density for the local NJL model, l3NJL. The hadronic parametrizations are GM1 and NL3, and the vector repulsion strengths are $G_V^L/G_S = 0$ and $G_V^L/G_S = 0.3$.

we consider the parameter sets GM1 and NL3. The quark phase is being investigated for repulsive vector interactions G_V among quarks which range from zero to the upper limits set by the local and non-local model. The equations of state shown in Figs. 2 and 3 are plotted

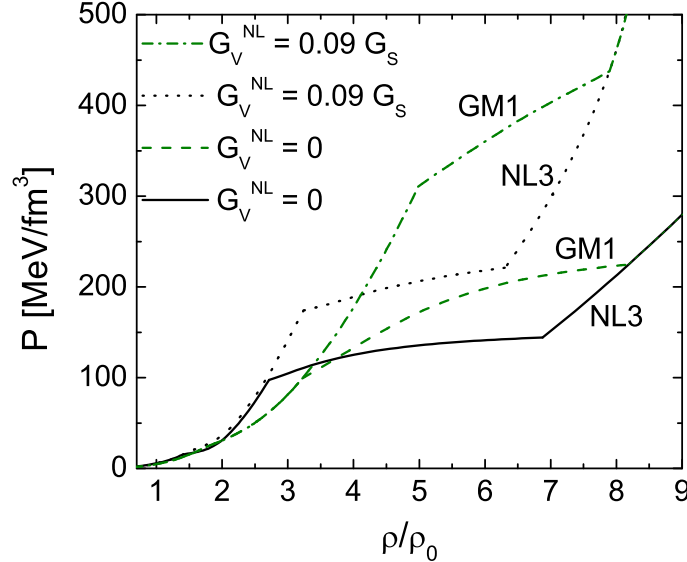


Figure 3. (Color online) Same as Fig. 2, but for the non-local NJL model, n3NJL, and vector repulsion strengths $G_V^{NL}/G_S = 0$ and $G_V^{NL}/G_S = 0.09$.

in the three-space spanned by the neutron chemical potential, electron chemical potential and pressure in Figs. 4 and 5.

Fig. 6 shows the mass-radius relationship of neutron stars for the three selected parametrizations of the hadronic lagrangian of this work. The transition to quark matter is included, but the vector repulsion among quarks is switched off. This lowers the maximum masses of the neutron stars (compare with Fig. 1), since a standard treatment of the quark-hadron transition softens the equation of state. The masses of the recently discovered high-mass neutron stars J1614-2230 ($1.97 \pm 0.04 M_\odot$) [14] and J0348+0432 ($2.01 \pm 0.04 M_\odot$) [15] are shown for comparison. Our calculations show that even for zero vector repulsion both stars could contain quark-hybrid matter in their cores.

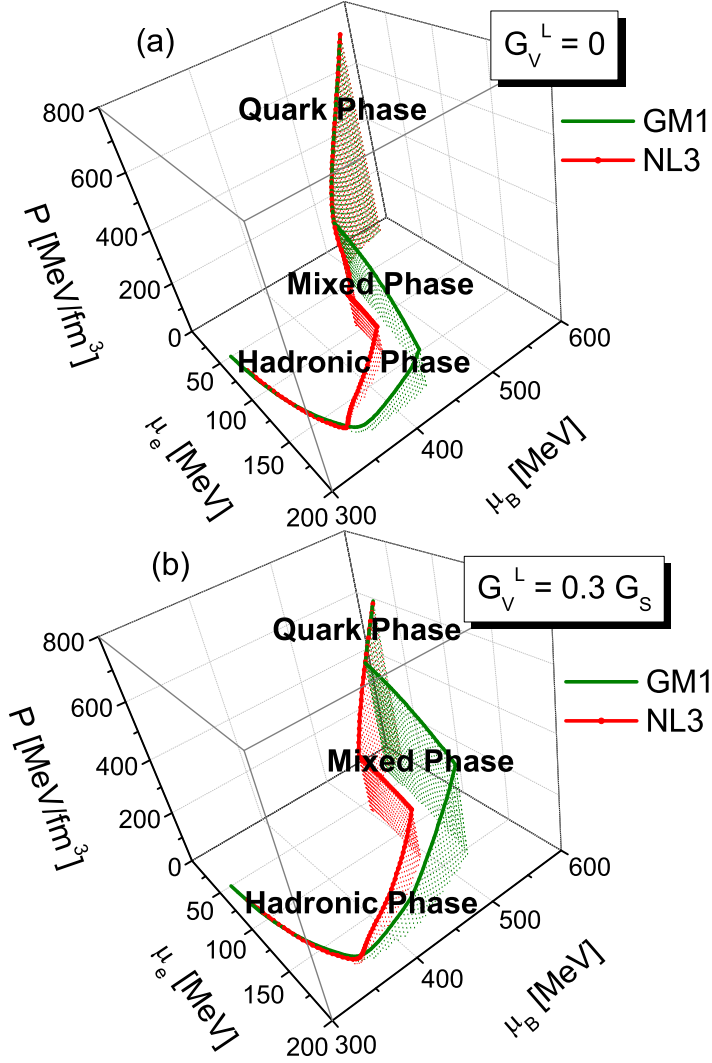


Figure 4. (Color online) Pressure as a function of baryon ($\mu_B = \mu_n/3$) and electron (μ_e) chemical potential for the local NJL model, l3NJL, hadronic parametrizations GM1 and NL3, and vector repulsions (a) $G_V^L/G_S = 0$ and (b) $G_V^L/G_S = 0.3$.

VI. QUARK-HYBRID COMPOSITION

In Figs. 7 through 10 we show the relative particle fractions Y_i ($\equiv \rho_i/\rho$) of neutron star matter as a function of baryon number density for both the local and non-local NJL model. It can be seen that by increasing the strength of the vector interaction, negatively charged particles like μ^- 's and Δ^- 's take on the role of electrons, whose primary duty is to make the stellar matter electrically neutral. Because of the early onset of the Δ population in our models, there is less need for electrons so that their number density in the mixed phase

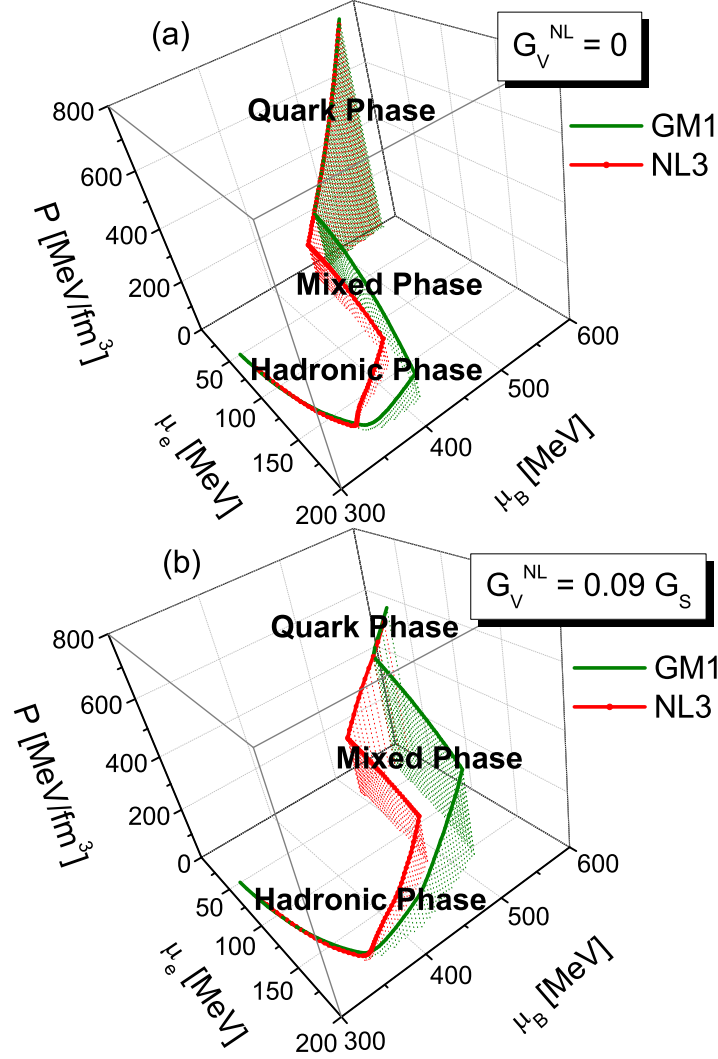


Figure 5. (Color online) Same as Fig. 4, but for the non-local NJL model, n3NJL, hadronic parametrizations GM1 and NL3, and vector repulsions (a) $G_V^{NL}/G_S = 0$ and (b) $G_V^{NL}/G_S = 0.09$.

is reduced compared to the outcome of standard mean-field/bag model calculations. Table V shows the densities beyond which leptons are no longer present in quark-hybrid matter (quark matter gets deleptonized). They are different for the local and non-local NJL model and depend on the ratio G_V/G_S .

Since we model the quark-hadron phase transition in three-space, accounting for the fact that the electric and baryonic charge are conserved for neutron star matter, the pressure varies monotonically with the proportion of the phases in equilibrium, as shown in Figs. 4 – 5 and 11 – 12. For the latter, the hatched areas denote the mixed phase regions where confined hadronic matter and deconfined quark matter coexist. The quark matter contents

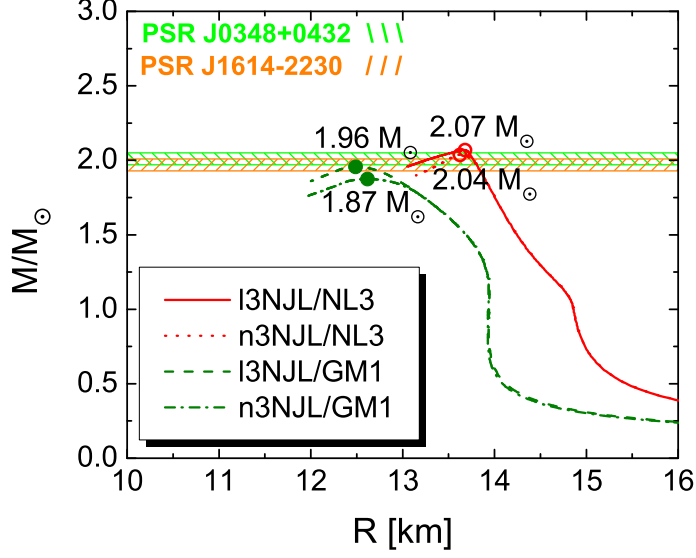


Figure 6. (Color online) Same as Fig. 1, but with quark matter included. The vector repulsion is $G_V = 0$.

Table V. Deleptonization densities for the local and non-local NJL model, for the GM1 parametrization ($\rho_0 = 0.16 \text{ fm}^{-3}$).

G_V/G_S	Deleptonization density (ρ_0)	
	Local NJL	Non-local NJL
0 (GM1)	6.65	5.85
0 (NL3)	6.61	4.55
0.09 (GM1)	—	7.03
0.09 (NL3)	—	5.33
0.30 (GM1)	7.45	—
0.30 (NL3)	6.26	—

of the maximum-mass neutron stars computed for these equations of state are indicated (χ values). Pure quark matter exists in stars marked with $\chi = 1$. Our calculations show that, in the non-local case, similarly to the observation in Ref. [16], the inclusion of the quark vector coupling contribution shifts the onset of the phase transition to higher densities and narrows the width of the mixed quark-hadron phase, when compared to the case $G_V = 0$.

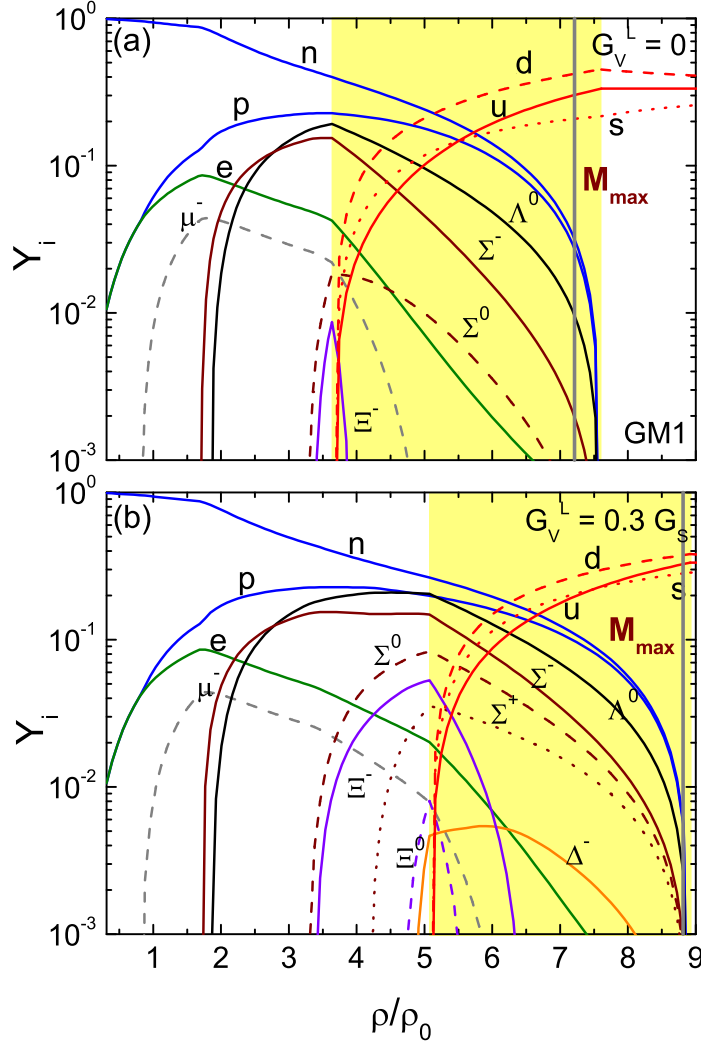


Figure 7. (Color online) Particle population of neutron star matter computed for the local NJL model, l3NJL. Yellow areas highlight the mixed phases. The solid vertical lines indicate the central densities of the associated maximum-mass NSs. The hadronic model parametrization is GM1 and the vector repulsions are (a) $G_V^L/G_S = 0$ and (b) $G_V^L/G_S = 0.3$.

To the contrary, when the quark matter phase is represented by the local l3NJL model, the width of the mixed phase tends to be broader for finite G_V values. This effect can be seen both in Fig. 11 as well as in Tables VI and VII.

To account for the uncertainty in the theoretical predictions of the ratio G_V/G_S [43, 50–52], we treat the vector coupling constant as a free parameter. We observed that the n3NJL model is more sensitive to the increase of G_V/G_S than the local model. For $G_V/G_S > 0.09$ we have a shift of the onset of the quark-hadron phase transition to higher and higher

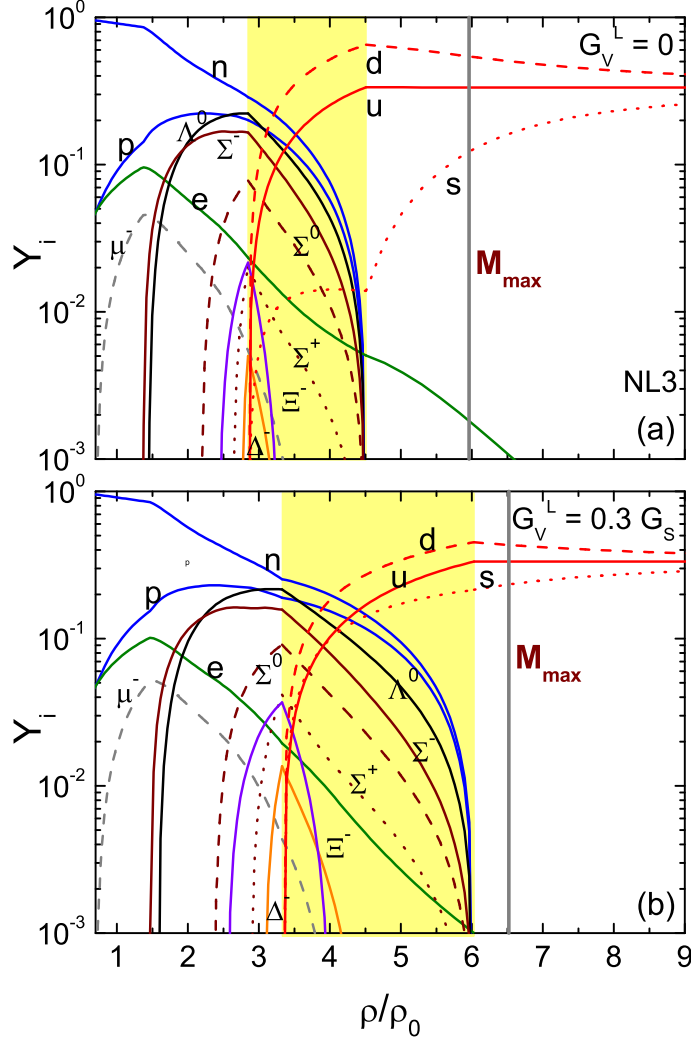


Figure 8. (Color online) Same as Fig. 7, but for the hadronic model parametrization NL3 and vector repulsions (a) $G_V^L/G_S = 0$ and (b) $G_V^L/G_S = 0.3$.

densities, preventing quark deconfinement in the cores of neutron stars. However, we can reach values of G_V/G_S up to 0.3 for the local NJL case.

Next we determine the bulk properties of spherically symmetric neutron stars for the collection of equations of state discussed in this paper. The properties are computed from the Tolmann-Oppenheimer-Volkoff (TOV) equation of general relativity theory [1, 2, 53]. The outcomes are shown in Figs. 13 and 14 for the local and non-local NJL model, respectively. The green and orange bands in Fig. 13 display the masses of the recently discovered, massive neutron stars PSR J1614-2230 [14] and J0348+0432 [15], respectively.

As a neutron star becomes increasingly more massive, the stellar core composition consist

Table VI. Widths of mixed phases and central densities of maximum-mass neutron stars for the local NJL model of this paper ($\rho_0 = 0.16 \text{ fm}^{-3}$).

G_V^L/G_S	Mixed phase	Central density of M_{max}
	(ρ_0)	(ρ_0)
0 (GM1)	3.64 – 7.60	7.21
0.30 (GM1)	5.07 – 8.92	8.81
0 (NL3)	2.85 – 4.51	5.96
0.30 (NL3)	3.33 – 6.03	6.52

Table VII. Widths of mixed phases and central densities of maximum-mass neutron stars for the non-local NJL model of this paper ($\rho_0 = 0.16 \text{ fm}^{-3}$).

G_V^{NL}/G_S	Mixed phase	Central density of M_{max}
	(ρ_0)	(ρ_0)
0 (GM1)	3.22 – 8.18	6.87
0.09 (GM1)	4.98 – 7.90	8.69
0 (NL3)	2.71 – 6.87	5.68
0.09 (NL3)	3.24 – 6.31	6.28

of either only nucleons, nucleons and hyperons, a mixed phase (MP) of quarks and hadrons, or a pure quark matter phase (QP), as indicated in Figs. 13 and 14. For the non-local NJL model and the NL3 parametrization for the hadronic phase (Fig. 14(b)), we find that pure quark does not exist in stable neutron stars. Only neutron stars which lie to the left of the mass peak are dense enough to contain such matter. These stars are however unstable against radial oscillations and thus cannot exist stably in the universe. The situation is different if the GM1 parameter set is used for the hadronic lagrangian. In this case a small amount of pure quark matter turns out to exist in the maximum-mass neutron star if the strength of the vector repulsion is non-zero ($G_V^{NL}/G_S = 0.09$). (See also Table VII.) Extended regions of a mixed phases of quarks and hadrons are found for both hadronic parametrizations. The situation is somewhat different for the local NJL model (Fig. 13), for which pure quark

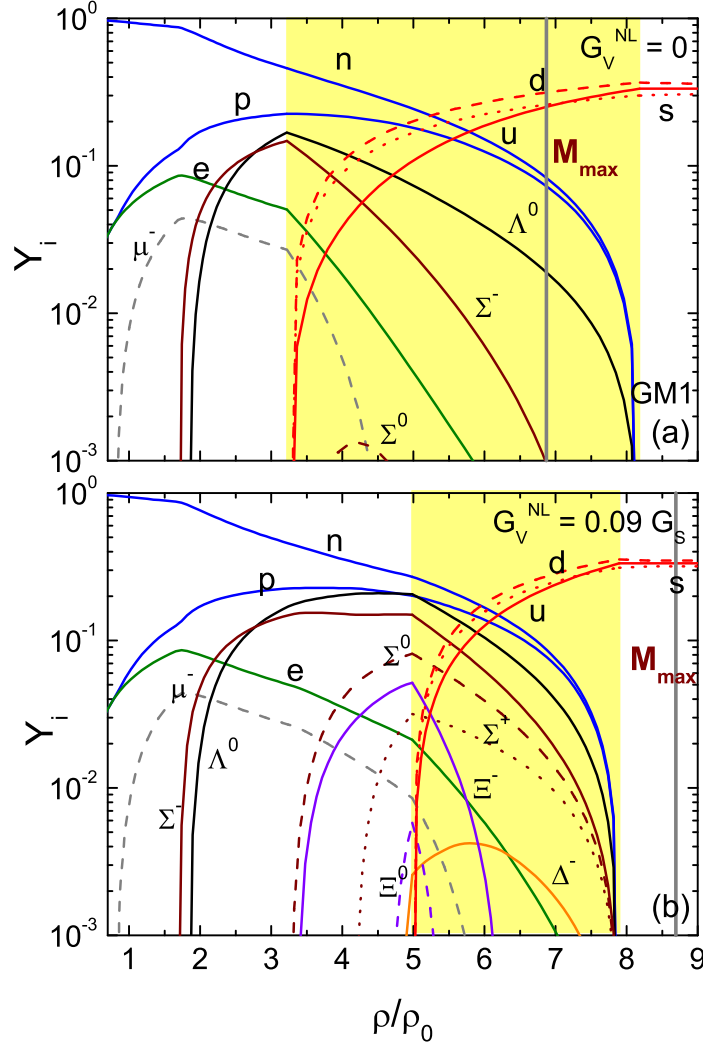


Figure 9. (Color online) Particle population of neutron star matter computed for the non-local NJL model, n3NJL. The yellow areas highlight the mixed phase. The solid vertical lines indicate the central densities of the associated maximum-mass NSs. The hadronic model parametrization is GM1 and the vector repulsions are (a) $G_V^{NL}/G_S = 0$ and (b) $G_V^{NL}/G_S = 0.09$.

matter cores are obtained for NL3 (see Table VI and Fig. 13(b)). The results for the masses and radii of the maximum-mass neutron stars are shown in Table VIII.

VII. SUMMARY AND CONCLUSIONS

In this work we use extensions of the local (l3NJL) and non-local (n3NJL) Nambu-Jona Lasinio model to analyze the possible occurrence of quark deconfinement in the cores of neu-

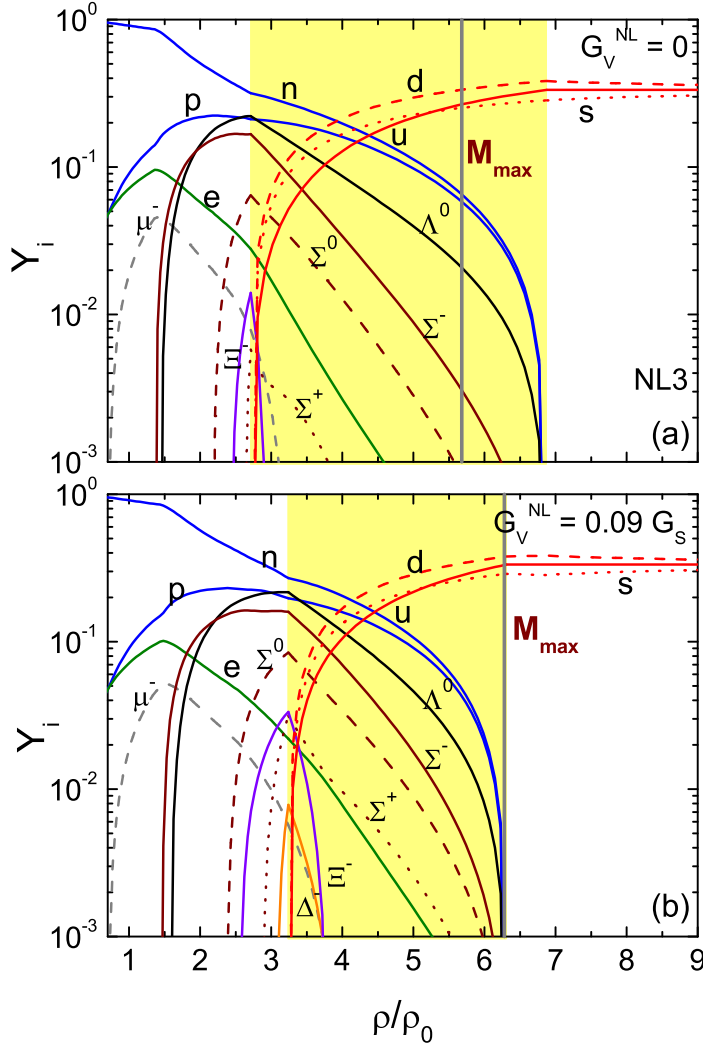


Figure 10. (Color online) Same as Fig. 9, but for the hadronic model parametrization NL3 and vector repulsions (a) $G_V^{NL}/G_S = 0$ and (b) $G_V^{NL}/G_S = 0.09$.

tron stars. We have constructed the phase transition from hadronic matter to quark matter via the Gibbs conditions, imposing global electric charge neutrality and baryon number conservation. We have calculated the mass-radius relationships of ordinary neutron stars and neutron stars with deconfined quarks in their centers (quark-hybrid stars). Depending on the strength of the quark vector repulsion, we find that mixed phases of confined hadronic matter and deconfined quarks can exist in neutron stars as massive as 2.1 to 2.4 M_\odot . The radii of these objects are between 12 and 13 km, as expected for neutron stars.

According to our study, for the n3NJL model, a transition to pure quark matter occurs only in neutron stars which lie on the gravitationally unstable branch of the stellar sequences

Table VIII. Maximum masses and radii of neutron stars made of quark-hybrid matter for different vector repulsion (G_V/G_S).

NJL Model	G_V/G_S	R_{max} (km)	M_{max}/M_{\odot}
Local	0	12.49	1.96
GM1	0.30	11.80	2.11
Local	0	13.68	2.07
NL3	0.30	13.53	2.37
Non-local	0	12.62	1.87
GM1	0.09	11.81	2.11
Non-local	0	13.62	2.04
NL3	0.09	13.56	2.35

if the parametrization NL3 for the hadronic matter lagrangian is used. This is different for the other hadronic parametrization considered in this paper, GM1, which predicts, for sufficiently large vector interactions among the quarks, pure quark matter cores in maximum-mass neutron stars. Pure quark matter cores are also obtained for the l3NJL model if the NL3 parametrization is being use. For the GM1 parametrization, however, pure quark matter is not present but gives way to an extended region of deconfined quarks which are in chemical equilibrium with various baryon species.

The latter is found to exist in all neutron stars models, independent of the value of the vector repulsion among quarks. With increasing stellar mass, all the stellar core compositions consist either of nucleons only, nucleons and hyperons, a mixed phase of quarks and hadrons (MP), and, in some cases, a pure quark matter phase (QP) in the core.

ACKNOWLEDGMENTS

M. Orsaria thanks N. N. Scoccola and T. Hell for helpful discussions. M. Orsaria and G. Contrera thank CONICET for financial support. H. Rodrigues thanks CAPES for financial support under contract number BEX 6379/10-9. F. Weber acknowledges supported by the National Science Foundation (USA) under Grant PHY-0854699.

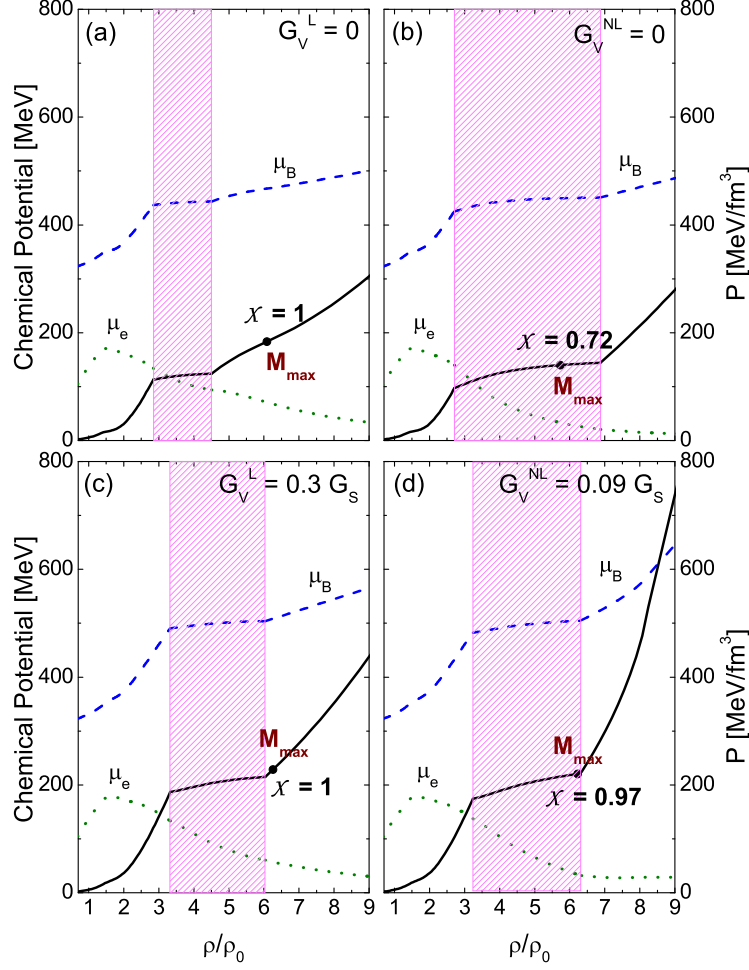


Figure 11. (Color online) Pressure P (solid lines), baryon chemical potential $\mu_B = \mu_n/3$ (dashed lines), and electron chemical potential μ_e (dotted lines) as a function of baryon number density (in units of $\rho_0 = 0.16 \text{ fm}^{-3}$) for parametrization NL3. The hatched areas denote the mixed phase regions where confined hadronic matter and deconfined quark matter coexist. Panels (a) and (b) are computed for l3NJL and n3NJL, respectively, and zero vector repulsion. The impact of finite values of the vector repulsion ($0.3G_S$ and $0.09G_S$) on the data is shown in panels (c) and (d) for l3NJL and n3NJL, respectively.

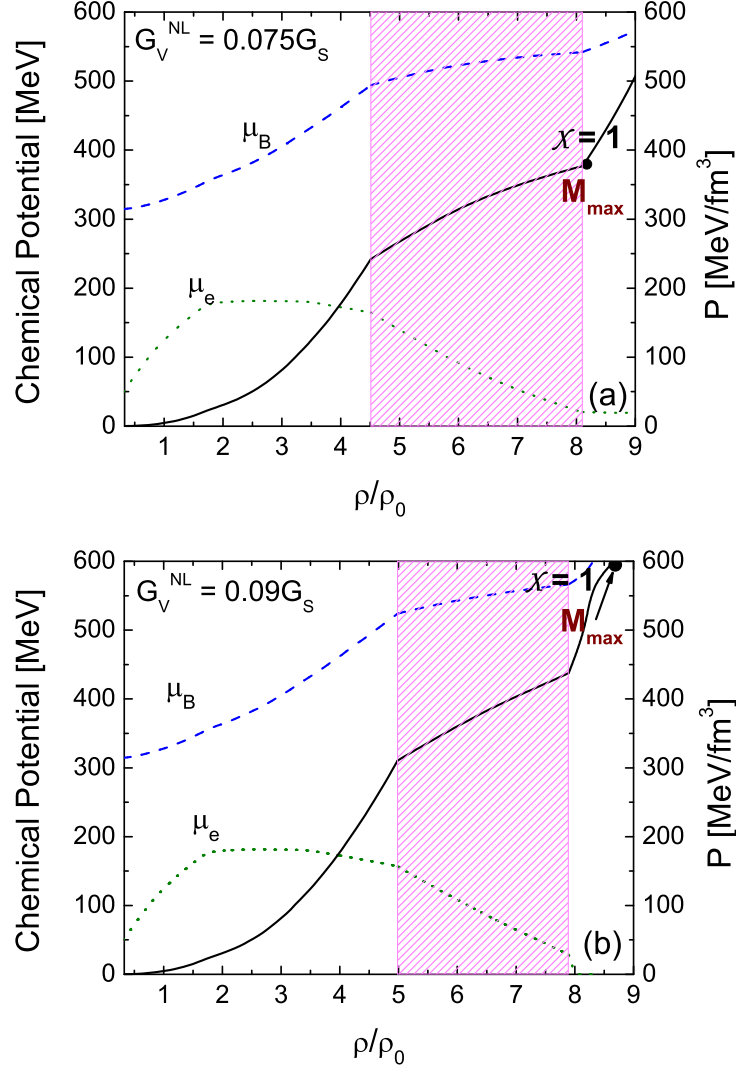
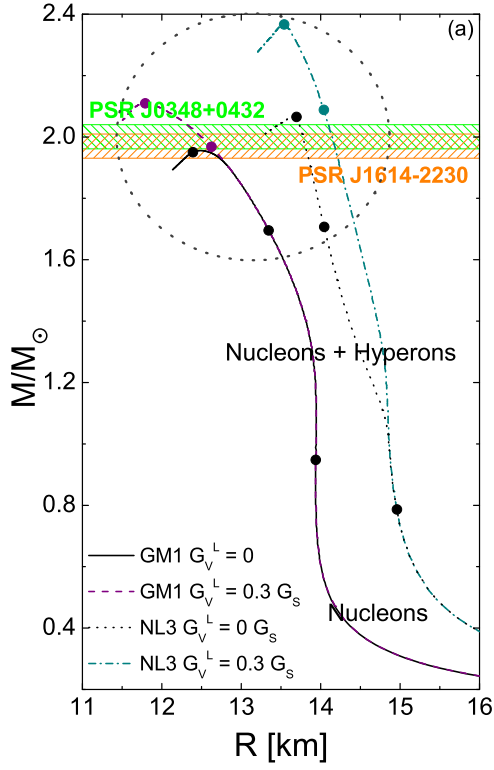
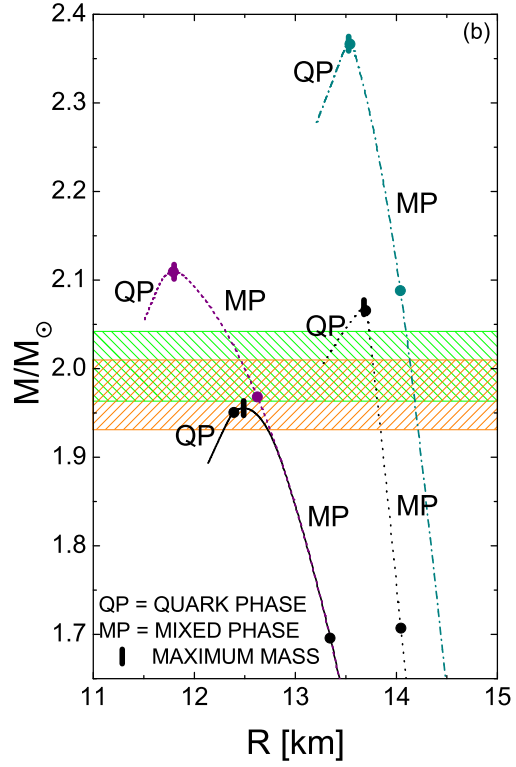


Figure 12. (Color online) Pressure P (solid lines), baryon chemical potential $\mu_B = \mu_n/3$ (dashed lines), and electron chemical potential μ_e (dotted lines) as a function of baryon number density (in units of $\rho_0 = 0.16 \text{ fm}^{-3}$) for parametrization GM1. The hatched areas denote mixed phase regions where confined hadronic matter and deconfined quark matter coexist. The data in panels (a) and (b) is for vector interactions $0.075G_S$ and $0.09G_S$, respectively.

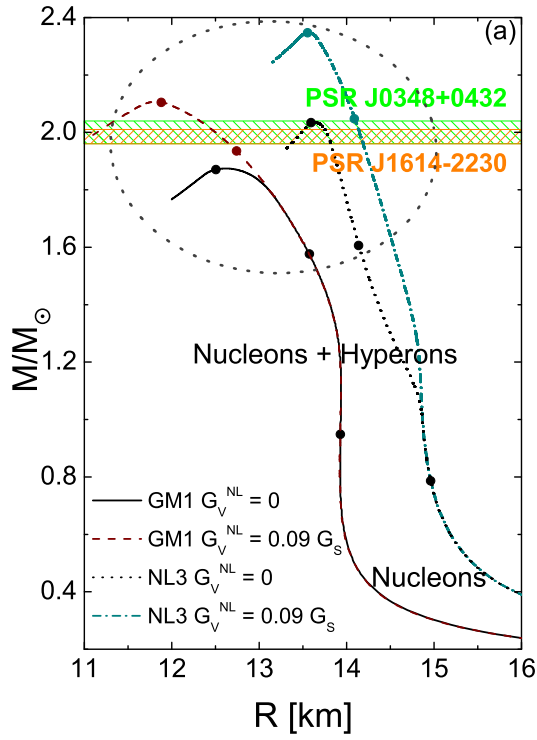


(a) Mass-radius relationships of neutron stars made of quark-hybrid matter.

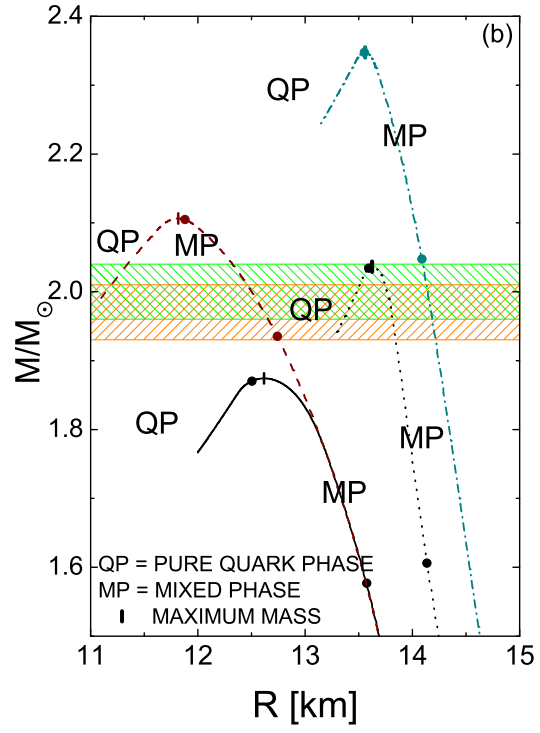


(b) Enlargement of the circled region of Fig. 13(a).

Figure 13. (Color online) Quark-hybrid matter inside of neutron stars, computed for the local NJL model (l3NJL) and hadronic model parametrizations GM1 and NL3. The symbols 'MP' and 'QP' stand for mixed phase and pure quark phase, respectively. The vertical bars denote the maximum-mass star of each stellar sequence.



(a) Mass-radius relationships of neutron stars made of quark-hybrid matter.



(b) Enlargement of the circled region of Fig. 14(a).

Figure 14. (Color online) Same as Fig. 13, but computed for the non-local NJL model (n3NJL) and hadronic model parametrizations GM1 and NL3.

-
- [1] N. K. Glendenning, *Compact Stars, Nuclear Physics, Particle Physics, and General Relativity*, 2nd ed. (Springer-Verlag, New York, 2000).
 - [2] F. Weber, *Pulsars as Astrophysical Laboratories for Nuclear and Particle Physics*, High Energy Physics, Cosmology and Gravitation Series (IOP Publishing, Bristol, Great Britain, 1999).
 - [3] *Physics of Neutron Star Interiors*, ed. by D. Blaschke, N. K. Glendenning and A. Sedrakian, Lecture Notes in Physics **578** (Spring-Verlag, Berlin, 2001).
 - [4] J. M. Lattimer and M. Prakash, *Astrophys. J.* **550**, 426 (2001).
 - [5] F. Weber, *Prog. Part. Nucl. Phys.* **54**, 193 (2005).
 - [6] D. Page and S. Reddy, *Ann. Rev. Nucl. Part. Sci.* **56**, 327 (2006).
 - [7] P. Haensel, A. Y. Potekhin and D. G. Yakovlev, *Neutron Stars 1*, Astrophysics and Space Science Library, (Springer-Verlag, New York, 2006).
 - [8] T. Klähn *et al.*, *Phys. Rev. C* **74**, 035802 (2006).
 - [9] A. Sedrakian, *Prog. Part. Nucl. Phys.* **58**, 168 (2007).
 - [10] T. Klähn *et al.*, *Phys. Lett. B* **654**, 170 (2007).
 - [11] M. G. Alford, A. Schmitt, K. Rajagopal and T. Schäfer, *Rev. Mod. Phys.* **80**, 1455 (2008).
 - [12] *Strongly Interacting Matter - The CBM Physics Book*, Lecture Notes in Physics **814** (Springer, 2011).
 - [13] I. Sagert, M. Wietoska and J. Schaffner-Bielich *J. Phys. G.* **32**, S241 (2006).
 - [14] P. B. Demorest, T. Pennucci, S. M. Ranson, M. S. E. Roberts and J. W. T. Hessels, *Nature* **467**, 1081 (2010).
 - [15] Lynch *et al.* *Astrophys. J.* **763**, 81 (2013); J. Antoniadis *et al.*, *Science* **340**, no. 6131 (2013).
 - [16] M. Orsaria, H. Rodrigues, F. Weber and G. A. Contrera, *Phys. Rev. D* **87**, 023001 (2013).
 - [17] Y. Nambu and G. Jona-Lasinio, *Phys. Rev.* **122**, 345 (1961); *Phys. Rev.* **124**, 246 (1961).
 - [18] G. Ripka, *Quarks bound by chiral fields* (Oxford University Press, Oxford, 1997).
 - [19] S. M. Schmidt, D. Blaschke and Yu. L. Kalinovsky, *Phys. Rev. C* **50**, 435 (1994).
 - [20] D. B. Blaschke, D. Gomez Dumm, A. G. Grunfeld, T. Klähn and N. N. Scoccola, *Phys. Rev. C* **75**, 065804 (2007).
 - [21] A. G. Grunfeld, J. Berdermann, D. B. Blaschke, D. Gomez Dumm, T. Klähn and N. N. Scoccola, *Int. J. Mod. Phys. E* **16**, 2842 (2007).

- [22] D. Blaschke, D. E. Alvarez Castillo, S. Benic, G. Contrera and R. Lastowiecki; PoS ConfinementX (2012) 249, arXiv:1302.6275 [hep-ph].
- [23] R. D. Bowler and M. C. Birse, Nucl. Phys. A **582**, 655 (1995); R. S. Plant and M. C. Birse, Nucl. Phys. A **628**, 607 (1998).
- [24] M. B. Parappilly, P. O. Bowman, U. M. Heller, D. B. Leinweber, A. G. Williams and J. B. Zhang, Phys. Rev. D **73**, 054504 (2006).
- [25] D. Blaschke, Yu L. Kalinovsky, G. Röpke, S. Schmidt and M. K. Volkov, Phys. Rev. C **53**, 2394 (1996).
- [26] G. A. Contrera, D. Gomez Dumm and N. N. Scoccola, Phys. Lett. B **661** 113 (2008).
- [27] G. A. Contrera, D. Gomez Dumm and N. N. Scoccola, Phys. Rev. D **81**, 054005 (2010).
- [28] T. Hatsuda and T. Kunihiro, Phys. Rep. **247**, 22 (1994).
- [29] P. Rehberg, S. P. Klevansky and J. Hufner, Phys. Rev. C **53**, 410 (1996).
- [30] C. Ratti, Europhys. Lett. **61**, 314 (2003).
- [31] G. Y. Shao, Phys. Lett. B **704**, 343 (2011).
- [32] M. Kitazawa, T. Koide, T. Kunihiro and Y. Nemoto, Prog. Theor. Phys. **108**, 929 (2002).
- [33] C. H. Lenzi and G. Lugones, Astrophys. J. **759**, 57 (2012).
- [34] L. Bonano and A. Sedrakian, A&A **539**, A16 (2012).
- [35] T. Endo, T. Maruyama, S. Chiba and T. Tatsumi, Prog. Theor. Phys. **115**, 337 (2006); T. Endo, arXiv:1310.0913 [astro-ph.HE].
- [36] N. K. Glendenning, Phys. Rev. D **46**, 1274 (1992).
- [37] N. K. Glendenning, Phys. Rep. **342**, 393 (2001).
- [38] D. Logoteta, C. Providência and I. Vidaña, Phys. Rev. C **88**, 055802 (2013).
- [39] K. Masuda, T. Hatsuda and T. Takatsuka, Astrophys. J. **764**, 12 (2013); K. Masuda, T. Hatsuda and T. Takatsuka, Prog. Theor. Exp. Phys. **2013** (2013) 073D01.
- [40] N. K. Glendenning and S. A. Moszkowski, Phys. Rev. Lett. **67**, 2414 (1991).
- [41] G. A. Lalazissis, J. König and P. Ring, Phys. Rev. C **55**, 540 (1997).
- [42] K. Kashiwa, T. Hell and W. Weise, Phys. Rev. D **84**, 056010 (2011).
- [43] G. A. Contrera, A. G. Grunfeld and D. B. Blaschke, arXiv:1207.4890 [hep-ph].
- [44] A. Scarpettini, D. Gomez Dumm and N. N. Scoccola, Phys. Rev. D **69**, 114018 (2004).
- [45] J. D. Walecka, Ann. Phys. **83**, 497 (1974).
- [46] B. D. Serot and J. D. Walecka, Adv. Nucl. Phys. **16**, 1 (1986).

- [47] S. Reddy, G. Bertsch and M. Prakash, Phys. Lett. B **475**, 1 (2000).
- [48] X. Na, R. Xu, F. Weber and R. Negreiros, Phys. Rev. D **86**, 123016 (2012).
- [49] M. Rotondo, Jorge A. Rueda, R. Ruffini and S.-S. Xue, Phys. Lett. B **701** 667 (2011).
- [50] C. Sasaki, B. Friman and K. Redlich, Phys. Rev. D **75**, 054026 (2007).
- [51] K. Fukushima, Phys. Rev. D **77**, 114028 (2008) [Erratum-ibid. Phys. Rev. D **78**, 039902 (2008)].
- [52] N. M. Bratovic, T. Hatsuda and W. Weise, Phys. Lett. B **719**, 131 (2013).
- [53] R. C. Tolman, Phys. Rev. **55**, 364 (1939); J. R. Oppenheimer and G. M. Volkoff, Phys. Rev. **55**, 374 (1939).